The Journal of Immunology

Cigarette Smoke-Induced Pulmonary Inflammation and Emphysema Are Attenuated in CCR6-Deficient Mice

Ken R. Bracke, An I. D'hulst, Tania Maes, Katrien B. Moerloose, Ingel K. Demedts, Serge Lebecque, Guy F. Joos and Guy G. Brusselle

J Immunol 2006; 177:4350-4359; ;
doi: 10.4049/jimmunol.177.7.4350
http://www.jimmunol.org/content/177/7/4350

The Journal of Immunology is published twice each month by
The American Association of Immunologists, Inc.,
1451 Rockville Pike, Suite 650, Rockville, MD 20852

Print ISSN: 0022-1767 Online ISSN: 1550-6606.

Cigarette Smoke-Induced Pulmonary Inflammation and Emphysema Are Attenuated in CCR6-Deficient Mice[1]

Ken R. Bracke,* An I. D'hulst,* Tania Maes,* Katrien B. Moerloose,* Ingel K. Demedts,* Serge Lebecque,† Guy F. Joos,* and Guy G. Brusselle[2]*

Chronic obstructive pulmonary disease (COPD) is mainly caused by cigarette smoking, and is characterized by an increase in inflammatory cells in the airways and pulmonary tissue. The chemokine receptor CCR6 and its ligand MIP-3α/CCL20 may be involved in the recruitment of these inflammatory cells. To investigate the role of CCR6 in the pathogenesis of COPD, we analyzed the inflammatory responses of CCR6 knockout (KO) and wild-type mice upon cigarette smoke (CS) exposure. Both subacute and chronic exposure to CS induced an increase in cells of the innate and adaptive immune system in the bronchoalveolar lavage, both in CCR6 KO and wild-type mice. However, the accumulation of dendritic cells, neutrophils, and T lymphocytes, which express CCR6, was significantly attenuated in the CCR6 KO mice, compared with their wild-type littermates. In the lung tissue of CCR6 KO mice, there was an impaired increase in dendritic cells, activated $CD8^+$ T lymphocytes, and granulocytes. Moreover, this attenuated inflammatory response in CCR6 KO mice offered a partial protection against pulmonary emphysema, which correlated with an impaired production of MMP-12. Importantly, protein levels of MIP-3α/CCL20, the only chemokine ligand of the CCR6 receptor, and MCP-1/CCL2 were significantly increased upon CS exposure in wild-type, but not in CCR6 KO mice. In contrast, CCR6 deficiency had no effect on the development of airway wall remodeling upon chronic CS exposure. These results indicate that the interaction of CCR6 with its ligand MIP-3α contributes to the pathogenesis of CS-induced pulmonary inflammation and emphysema in this murine model of COPD. *The Journal of Immunology,* **2006, 177: 4350–4359.**

Chronic obstructive pulmonary disease (COPD)[3] is one of the leading causes of mortality and morbidity in the world, and its prevalence is expected to increase in the next decades (1, 2). The disease is characterized by a slowly progressive development of airflow limitation that is poorly reversible. The airflow limitation is due to chronic obstructive bronchiolitis and loss of elastic recoil caused by destruction of lung parenchyma (emphysema) (3). Patients with COPD also display pathologically distinct structural alterations of the small airways (airway remodeling) (4), as well as systemic inflammation (5, 6). The molecular and cellular mechanisms that are responsible for the development of COPD are not well understood. Cigarette smoking is the major risk factor for the development of COPD, and it has been shown that chronic exposure to cigarette smoke (CS) leads to lung inflammation with an increase of inflammatory cells such as macrophages (7, 8), neutrophils (9, 10), dendritic cells (DCs) (11, 12), and $CD8^+$ T lymphocytes (13). These cells are capable of releasing inflammatory mediators and proteinases, such as matrix metalloproteinases (MMPs) or neutrophil elastase, which are believed to play a role in the progressive lung destruction in COPD (14–16).

Several cytokines and chemokines are assumed to regulate the activation and recruitment of these inflammatory cells into the airways and pulmonary tissue of COPD patients. For example, it has been described that binding of MCP-1 to its receptor CCR2 leads to recruitment of DCs and monocytes from the blood to the tissue (17) and that IL-8 (or the mouse homolog KC) is chemotactic for neutrophils (18). In recent papers, some investigators suggested that COPD is an autoimmune disease triggered by CS (19, 20), which would then depend heavily on the presence of T lymphocytes and DCs. Moreover, in patients with severe COPD (Global Initiative for Obstructive Lung Disease stages 3 and 4), lymphoid follicles containing T and B lymphocytes are present in the peribronchial wall (21). Recently, in a murine model of CS-induced COPD (22), we and others (23, 24) have described a significant increase in the number and size of peribronchial follicles upon chronic CS exposure.

Chemokines are a family of structurally related chemotactic proteins, whose primary role is to direct the migration of leukocytes throughout the body, both under physiological and inflammatory conditions. Moreover, they have broad-reaching effects on other fundamental aspects of immunology, including the development, homeostasis, and function of the immune system. Generally, chemokines exert their biological functions by interaction with specific chemokine receptors on their target cells (25).

Chemokine receptor CCR6, a seven-transmembrane-domain G protein-coupled receptor, is a receptor that, unlike most of its family members, has only one chemokine ligand, namely MIP-3α (CCL20). It has, however, been described that certain members of the β-defensin family also bind CCR6, but with lower affinity (26). CCR6 is expressed on immature DCs (27), B lymphocytes (28), memory T cells (29), cytokine-activated neutrophils (30), and at

*Department of Respiratory Diseases, Ghent University Hospital, Ghent, Belgium; and †Service de Pneumologie, Centre Hospitalier Universitaire-Lyon, France

Received for publication February 17, 2006. Accepted for publication July 13, 2006.

The costs of publication of this article were defrayed in part by the payment of page charges. This article must therefore be hereby marked *advertisement* in accordance with 18 U.S.C. Section 1734 solely to indicate this fact.

[1] This work was supported by the Fund for Scientific Research in Flanders (Fonds Wetenschappelijk Onderzoek Vlaanderen, Research Project G.0011.03), the Strategic Basic Research (Strategisch Basisonderzoek-Instituut voor de Aanmoediging van Innovatie door Wetenschap en Technologie in Vlaanderen/020203), and the Concerted Research Action of the University of Ghent (BOF/GOA 01251504).

[2] Address correspondence and reprint requests to Dr. Guy G. Brusselle, Department of Respiratory Diseases, Ghent University Hospital 7K12ie, De Pintelaan 185, 9000 Ghent, Belgium. E-mail address: guy.brusselle@UGent.be

[3] Abbreviations used in this paper: COPD, chronic obstructive pulmonary disease; BAL, bronchoalveolar lavage; CBA, cytometric bead array; CS, cigarette smoke; DC, dendritic cell; DI, destructive index; hprt, hypoxanthine guanine phosphoribosyltransferase; KO, knockout; L_m, mean linear intercept; MMP, matrix metalloproteinase; Pbm, length of the basement membrane.

0022-1767/06/$02.00

low levels on endothelial cells (31). The MIP-3α/CCR6 interaction functions as one of the most potent mechanisms for recruitment of immature DC (32, 33). MIP-3α is expressed predominantly in inflamed epithelial surfaces, including the airway epithelium (34), and could thus regulate the migration of immature DCs to the airways for subsequent Ag presentation. It has also been reported that MIP-3α is chemotactic for T lymphocytes (35). Moreover, MIP-3α expression can be up-regulated by a broad spectrum of proinflammatory cytokines (e.g., TNF-α) and by ambient particles (34), making it an ideal candidate for a role in chronic inflammatory airway diseases such as COPD. CCR6 has also been implicated in asthma, in which it has been shown that CCR6 knockout (KO) mice have a reduced allergic pulmonary inflammation in response to cockroach Ag (36).

These data suggest that CCR6 and its ligand MIP-3α may play a role in the inflammatory cell recruitment in COPD. To elucidate the functional role of CCR6 in the pathogenesis of COPD, we tested CCR6 KO and wild-type mice in a model of CS-induced pulmonary inflammation and emphysema (22). We analyzed the inflammatory responses in both bronchoalveolar lavage (BAL) and lung tissue after subacute (4-wk) or chronic (24-wk) exposure to CS. Second, we quantified the extent of pulmonary emphysema, airway wall remodeling, and peribronchial aggregates in both CCR6 KO and wild-type mice upon chronic CS exposure.

Materials and Methods

Animals

A breeding pair of mice with disruption of the CCR6 gene was obtained from S. Lebecque (Service de Pneumologie, Centre Hospitalier Universitaire-Lyon, France). The CCR6 KO mice were backcrossed 10 generations onto the C57BL/6 background (37). Male CCR6 KO mice were bred (8 wk old) and male C57BL/6 wild-type mice (8 wk old) were used as control mice (Charles River Laboratories). The local ethics committee for animal experimentation of the faculty of Medicine and Health Sciences (Ghent, Belgium) approved all in vivo manipulations.

CS exposure

Mice ($n = 8$) were exposed whole body to CS, as described previously (22). Briefly, groups of eight mice were exposed to the tobacco smoke of five cigarettes (Reference Cigarette 2R4F without filter; University of Kentucky) four times per day with a 30-min smoke-free interval, 5 days per week for 4 wk (subacute exposure) or 24 wk (chronic exposure). An optimal smoke:air ratio of 1:6 was obtained. The control groups were exposed to air. Carboxyhemoglobin in serum of smoke-exposed mice reached a nontoxic level of 8.3 ± 1.4% (compared with 1.0 ± 0.2% in air-exposed mice ($n = 7$ for both groups)), which is similar to carboxyhemoglobin blood concentrations of human smokers (38).

Bronchoalveolar lavage

Twenty-four hours after the last exposure, mice were weighed and sacrificed with an overdose of pentobarbital (Sanofi-Synthelabo), and a tracheal cannula was inserted. A total of 3 × 300 μl, followed by 3 × 1 ml of HBSS, free of ionized calcium and magnesium, but supplemented with 0.05 mM sodium EDTA, was instilled via the tracheal cannula and recovered by gentle manual aspiration. The six lavage fractions were pooled and centrifuged, and the cell pellet was washed twice and finally resuspended in 1 ml of HBSS. A total cell count was performed in a Bürcker chamber, and the differential cell counts (on at least 400 cells) were performed on cytocentrifuged preparations using standard morphologic criteria after May-Grünwald-Giemsa staining. Flow cytometric analysis of BAL cells was performed to enumerate DCs and $CD4^+$ and $CD8^+$ T lymphocytes.

Collection of blood leukocytes

Following BAL, blood was drawn by cardiac puncture and collected in EDTA-coated tubes. The blood was subjected to RBC lysis and labeled for differential leukocyte counts by flow cytometry.

Preparation of lung single-cell suspensions

Following cardiac puncture, the pulmonary and systemic circulation was rinsed. The left lung was used for histology, and the right lung for the preparation of a cell suspension, as detailed previously (39). Briefly, the lung was thoroughly minced, digested, subjected to RBC lysis, passed through a 50-μm cell strainer, and kept on ice until labeling. Cell counting was performed with a Z2 Beckman Coulter particle counter (Beckman Coulter).

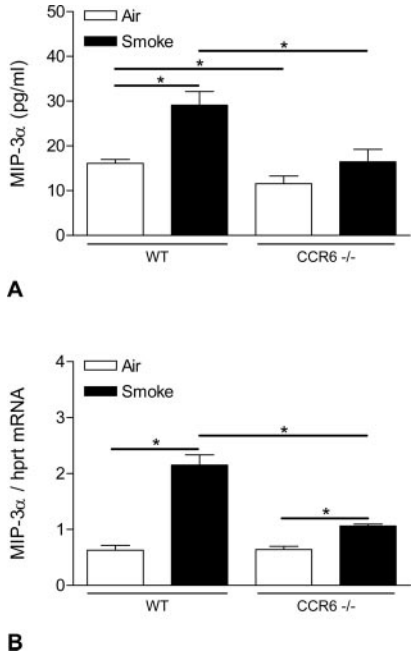

FIGURE 1. Measurement of MIP-3α in BAL fluid and lung tissue. *A*, Protein levels of MIP-3α/CCL20 in the BAL fluid of wild-type and CCR6 KO mice after subacute (4-wk) exposure to air or CS, as measured by ELISA. Results are expressed as pg/ml (mean ± SEM). $n = 8$ animals/group; ∗, $p < 0.05$. *B*, mRNA levels of MIP-3α/CCL20 in total lung tissue of wild-type and CCR6 KO mice after subacute (4-wk) exposure to air or CS, as measured by RT-PCR. Results are expressed as a ratio with hprt mRNA (mean ± SEM). $n = 5$ animals/group; ∗, $p < 0.05$.

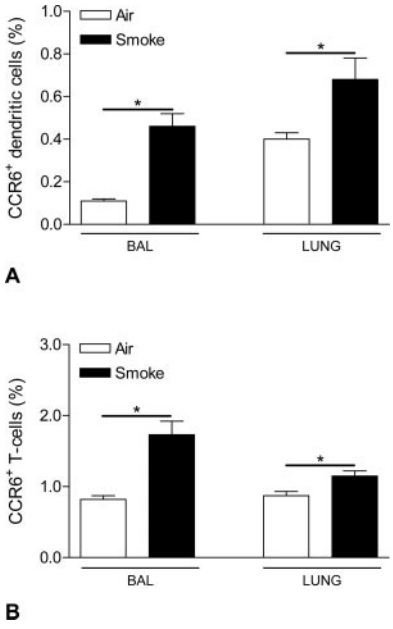

FIGURE 2. CCR6-expressing DCs (*A*) and T lymphocytes (*B*) in BAL fluid and lung digests of wild-type mice after subacute (4-wk) exposure to air or CS, enumerated by flow cytometry. Results are expressed as percentage of total cells (means ± SEM). $n = 8$ animals/group; ∗, $p < 0.05$.

Labeling of BAL cells, lung single-cell suspensions, and blood leukocytes for flow cytometry

Cells were preincubated with FcR blocking Ab (anti-CD16/CD32, clone 2.4G2) to reduce nonspecific binding. The following mAbs were used to identify mouse DC populations: biotinylated anti-CD11c (N418) and PE-conjugated anti-I-A^b (AF6-120.1). We discriminated between macrophages and DCs using the methodology described by Vermaelen and Pauwels (40). After gating on the CD11c-bright population, two peaks of autofluorescence can be distinguished. Macrophages are identified as the CD11c-bright, high autofluorescent population, and do not express MHC class II. DCs are identified as CD11c-bright, low autofluorescent cells, which strongly express MHC class II. DCs enumerated by these criteria correspond with myeloid DCs. The following Abs were used to stain mouse T cell subpopulations: FITC-conjugated anti-CD4 (L3T4), FITC-conjugated anti-CD8 (Ly-2), and biotinylated anti-CD3 (145-2C11) mAbs. The additional marker used for T cell activation was PE-conjugated anti-CD69 (H1.2F3). PE-conjugated anti-CD19 (1D3) and anti-CD11c were used to characterize B lymphocytes. PE-conjugated anti-GR1 (Ly-6G) and biotinylated anti-CD11c Abs were used to characterize pulmonary granulocytes. The following Abs were used to differentiate blood leukocytes: FITC-conjugated anti-CD11b (M1/70), PE-conjugated anti-CD45 (Ly-5), allophycocyanin-conjugated anti-CD3, and biotinylated anti-CD19. CCR6 expression was revealed with PE-conjugated anti-CCR6 (140706). Biotinylated anti-CD11c and anti-CD3 were revealed by incubation with streptavidin-allophycocyanin. Biotinylated anti-CD19 was revealed by incubation with streptavidin-PerCP. All mAbs were obtained from BD Pharmingen, except anti-CD11c (N418 hybridoma; a gift from M. Moser, Brussels Free University, Brussels, Belgium) and anti-CCR6 (R&D Systems).

As a last step before analysis, cells were incubated with 7-aminoactinomycin D (or viaprobe; BD Pharmingen) for dead cell exclusion. All labeling reactions were performed on ice in FACS-EDTA buffer.

Flow cytometry data acquisition was performed on a dual-laser FACS-Vantage flow cytometer running CellQuest software (BD Biosciences). FlowJo software (⟨www.Treestar.com⟩) was used for data analysis.

Histology

The left lung was fixated by gentle infusion of fixative (4% paraformaldehyde) through the tracheal cannula (22). After excision, the lung was immersed in fresh fixative during 2 h. The lung lobe was embedded in paraffin and cut in 3-μm transversal sections. Lung tissue samples were stained with H&E and examined by light microscopy for histological sections. For each animal, 10 fields at a magnification of $\times$200 were captured in a blinded fashion using a Zeiss KS400 image analyzer platform (KS400; Zeiss).

Quantification of emphysema

Emphysema is a structural disorder characterized by destruction of the alveolar walls and enlargement of the alveolar spaces. We determined destruction of alveolar walls by measuring the destructive index (DI) (41) and

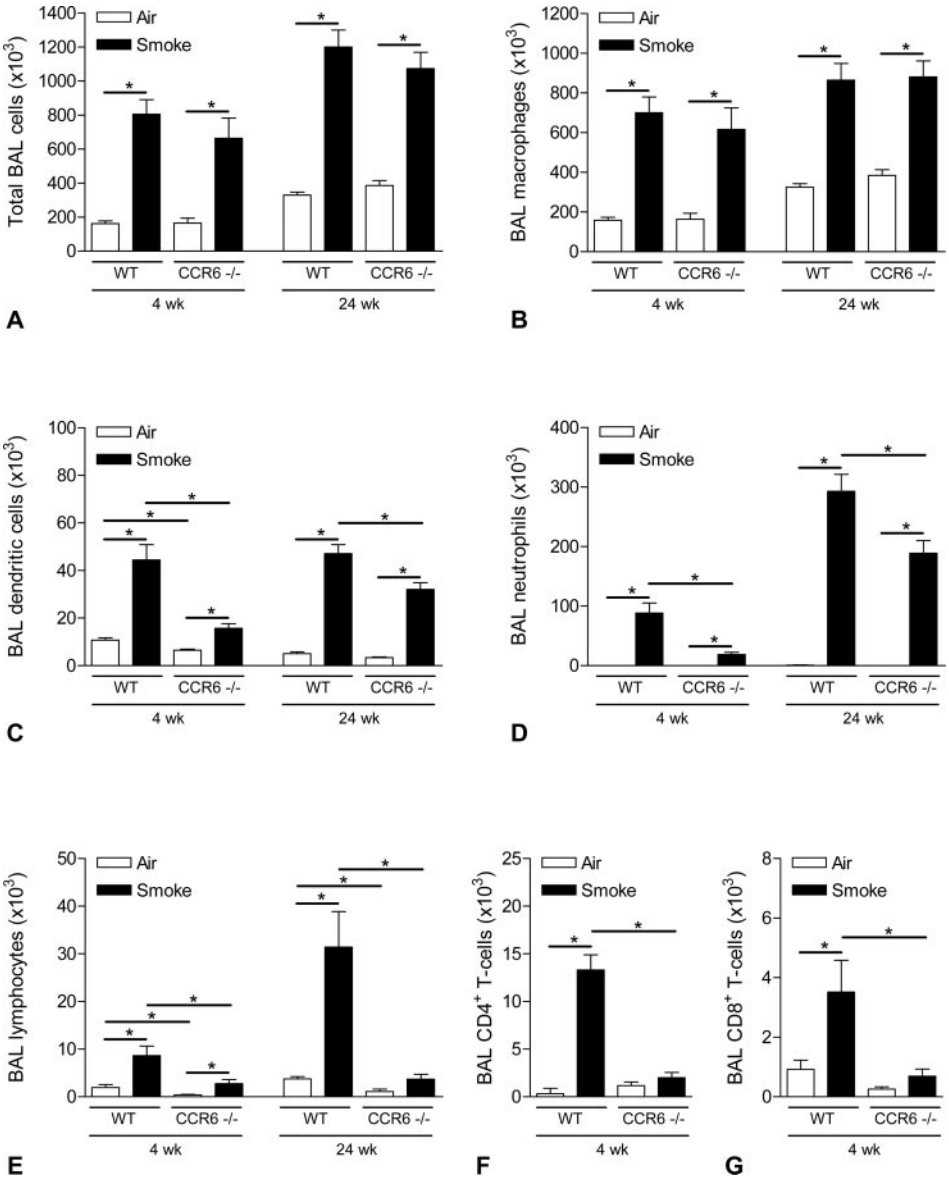

FIGURE 3. Total BAL cells and cell differentiation in BAL fluid of wild-type and CCR6 KO mice after subacute (4-wk) or chronic (24-wk) exposure to air or CS: *A*, total BAL cells; *B*, macrophages; *C*, DCs; *D*, neutrophils; *E*, lymphocytes; *F*, $CD4^+$ T lymphocytes; and *G*, $CD8^+$ T lymphocytes (*A*, *B*, *D*, and *E* were calculated on cytospins; *C*, *F*, and *G* were enumerated by flow cytometry). Results are expressed as means $\pm$ SEM. $n = 8$ animals/group; $*$, $p < 0.05$.

enlargement of alveolar spaces by quantifying the mean linear intercept (L_m) (42), as described previously (22, 23).

Quantification of airspace enlargement was determined after 6-mo air or CS exposure by measuring the L_m using image analysis software (Image J 1.33). The L_m was measured by placing a 100 × 100-μm grid over each field. The total length of each line of the grid divided by the number of alveolar intercepts gives the average distance between alveolated surfaces, or the L_m (42).

The destruction of alveolar walls was quantified by the DI (41). A grid with 42 points that were at the center of hairline crosses was superimposed on the lung field. Structures lying under these points were classified as normal (N) or destroyed (D) alveolar and/or duct spaces. Points falling over other structures, such as duct walls, alveolar walls, etc., did not enter into the calculations. The DI was calculated from the formula: DI = D/(D + N) × 100.

Morphometric quantification of lymphoid aggregates

To evaluate the presence of lymphoid aggregates in lung tissue after 6-mo air or CS exposure, lung sections obtained from Formalin-fixed, paraffin-embedded lung lobes were subjected to an immunohistological CD3 staining: at first, sections were incubated with Boehringer blocking reagent with Triton X-100 and primary Ab anti-CD3, followed by goat anti-rabbit biotin (both obtained from DakoCytomation). Then, slides were incubated with streptavidin HRP and colored with diaminobenzidine (both obtained from DakoCytomation). Lymphoid aggregates were defined as accumulations of at least 50 cells and counted in the tissue area surrounding the airways (airway perimeter 0–2000 μm). Results were expressed as counts relative to the numbers of airways per lung section.

Measurement of chemokines and cytokines

Using a commercially available ELISA kit (R&D Systems), MIP-3α protein level was determined in BAL fluid after 4 and 24 wk of air or CS exposure.

At the same time points, cytokines and chemokines in BAL fluid were determined by FACS using the cytometric bead array (CBA; BD Biosciences), following the manufacturer's instructions. A mixture of three capture bead populations, each with distinct fluorescence intensities and coated with Abs specific for TNF-α, MCP-1, and KC, was prepared. The CBA capture beads were incubated together with PE-conjugated detection Abs and test samples or standards, to form sandwich complexes. Following acquisition of sample data using the flow cytometer (FACSCalibur flow cytometer; BD Biosciences), the sample results were generated in graphical and tabular format using the CBA Analysis Software (BD Biosciences).

Immunohistochemistry for MMP-12

Sections obtained from Formalin-fixed, paraffin-embedded lung lobes were subjected to the following immunohistological staining sequences: blocking reagent, goat anti-mouse MMP-12 (Santa Cruz Biotechnology), or goat IgG isotype control, and detection with Vectastain Elite Goat IgG ABC Kit (Vector Laboratories) and diaminobenzidine substrate (DakoCytomation). Sections were counterstained with hematoxylin.

RT-PCR analysis

Total lung RNA was extracted with the RNeasy Midi Kit (Qiagen). Expression of MIP-3α, MMP-12, and TNF-α mRNA, relative to hypoxanthine guanine phosphoribosyltransferase (hprt) mRNA, was analyzed with the Assays-on-Demand Gene Expression Products (Applied Biosystems).

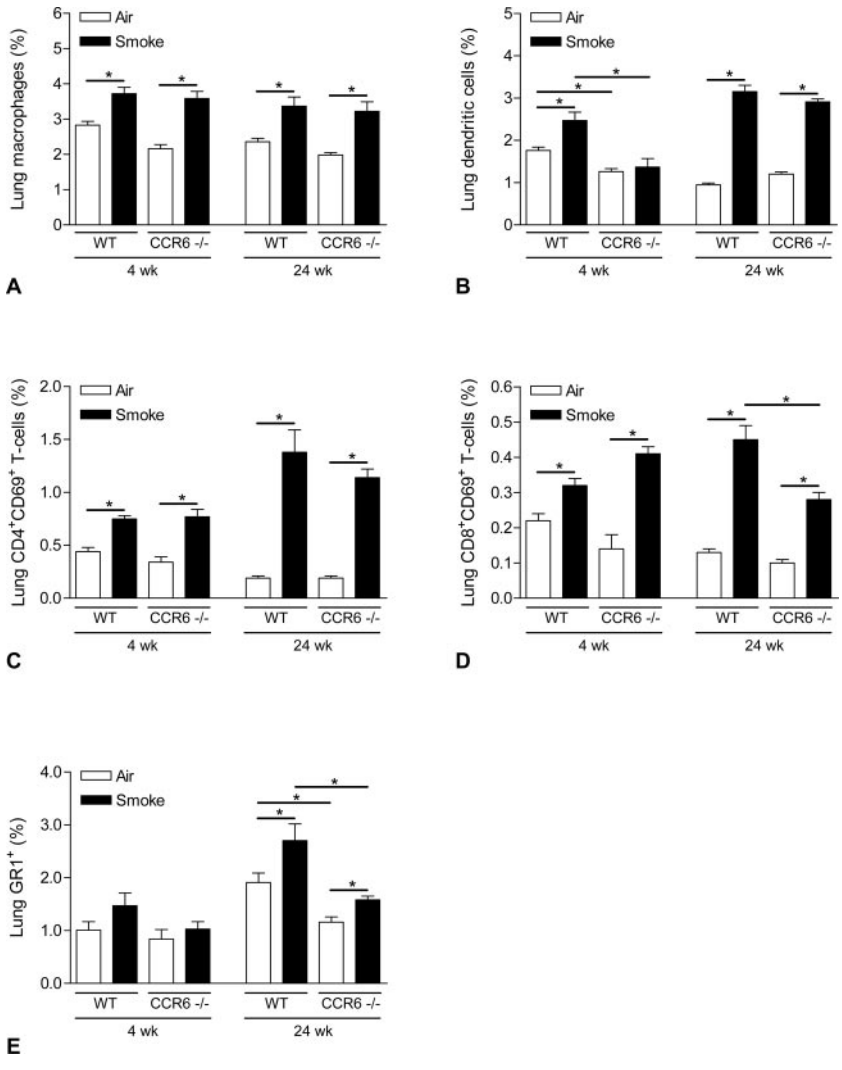

FIGURE 4. Cell differentiation in the lungs of wild-type and CCR6 KO mice after subacute (4-wk) or chronic (24-wk) exposure to air or CS: *A*, macrophages; *B*, DCs; *C*, activated $CD4^+$ T lymphocytes; *D*, activated $CD8^+$ T lymphocytes; and *E*, granulocytes (all cell types were enumerated by flow cytometry). Results are expressed as means ± SEM. $n = 8$ animals/group; $*$, $p < 0.05$.

RT-PCR was performed on an ABI PRISM 7700 Sequence Detection System with murine leukemia virus RTase (Applied Biosystems). Reverse transcription was performed at 48°C for 30 min, followed by 12-min incubation at 95°C for denaturation of RNA-DNA heteroduplexes, and 50 cycles of 95°C for 15 s and 60°C for 60 s. Monitoring of the RT-PCR occurred in real time using a FAM/TAMRA probe. All reactions were performed starting from 10 ng of total RNA.

Airway remodeling

Collagen in the airway wall was stained using Sirius Red, and the amount of fibronectin with a goat anti-rat fibronectin Ab (Calbiochem) using the streptavidin-biotin peroxidase method (43). For each experimental group, three lung sections per animal were examined. Morphometrical parameters (44) were marked manually on the digital representation of the airway: the length of the basement membrane (Pbm), the area defined by the basement membrane (Abm), and the area defined by the total adventitial perimeter (Ao). The total bronchial wall area (WAt) was calculated (WAt = Ao – Abm) and normalized to the squared Pbm. For the quantification of collagen and fibronectin deposition, the area in the airway wall covered by the stain was determined by the software (KS400; Zeiss) and its value was calculated, as described previously (43). The area of collagen or fibronectin deposition was normalized to Pbm. All airways with a Pbm smaller than 2000 μm and cut in reasonable cross sections (defined by a ratio of minimal to maximal internal diameter >0.5) were included.

Statistical analysis

Reported values are expressed as mean ± SEM. Statistical analysis was performed with Sigma Stat software (SPSS) using nonparametric tests (Kruskall-Wallis; Mann-Whitney *U*). A p value <0.05 was considered significant.

Results

Increased MIP-3α/CCL20 levels in the BAL fluid and lungs upon subacute CS exposure

Because MIP-3α is the only known chemokine ligand for CCR6, we examined the presence of MIP-3α protein in the BAL fluid of wild-type and CCR6 KO mice by ELISA. Subacute (4-wk) exposure to CS significantly increased the levels of MIP-3α in the BAL fluid of wild-type mice, compared with air-exposed littermates. In contrast, we did not observe a CS-induced up-regulation of MIP-3α protein in CCR6 KO mice (Fig. 1*A*). Moreover, the amounts of MIP-3α were significantly lower in both air- and CS-exposed CCR6 KO mice, compared with wild-type animals (Fig. 1*A*).

RT-PCR analysis on RNA extracted from total lung tissue also revealed a significant increase of MIP-3α expression upon CS exposure. Again, this time on the mRNA level, there was significantly less expression in the CS-exposed CCR6 KO mice, compared with wild-type mice (Fig. 1*B*).

Subacute CS-induced increase of CCR6-expressing DCs and T lymphocytes

FACS analysis using an anti-CCR6 mAb clearly revealed CCR6 expression on DCs and T lymphocytes of wild-type mice. Upon subacute CS exposure, there was, in both BAL and lung tissue, a significant increase in CCR6-expressing DCs and T lymphocytes, measured as percentage of total cells (Fig. 2). The CCR6 expression within the DC population also increased upon CS exposure in both BAL (air, 5.52 ± 0.70% vs smoke, 8.20 ± 0.85%) and lung tissue (air, 22.41 ± 1.30% vs smoke, 27.07 ± 2.68%), but this did not reach statistical significance (data not shown). The CCR6 expression within the T lymphocyte population did not change in lung tissue (air, 48.60 ± 3.49% vs smoke, 48.70 ± 3.96%) and even tended to decrease in BAL (air, 43.74 ± 3.15% vs smoke, 32.83 ± 2.42%) (data not shown).

CS-induced increase of inflammatory cells in the BAL fluid

Subacute and chronic exposure to CS increased the absolute numbers of total cells, alveolar macrophages, DCs, lymphocytes, and neutrophils in the BAL fluid of both wild-type and CCR6 KO mice, compared with air-exposed animals (Fig. 3). There were no significant differences in total numbers of BAL cells and alveolar macrophages between wild-type and CCR6 KO mice upon CS exposure (Fig. 3, *A* and *B*). In contrast, at both time points (4 and 24 wk), the numbers of DCs, lymphocytes, and neutrophils were significantly lower in the CS-exposed CCR6 KO mice, compared with wild-type animals (Fig. 3, *C–E*). Within the lymphocyte population, the CS-induced accumulation of both $CD4^+$ and $CD8^+$ cells was attenuated in CCR6 KO mice (Fig. 3, *F* and *G*).

Moreover, baseline levels of BAL DCs and lymphocytes were significantly lower in air-exposed CCR6 KO mice, compared with their wild-type littermates (Fig. 3, *C* and *E*).

CS-induced increase of inflammatory cells in the lungs

In lung single-cell suspensions, subacute and chronic exposure to CS induced an increase in interstitial macrophages, DCs, activated $CD4^+$ and $CD8^+$ T lymphocytes, and granulocytes in both wild-type and CCR6 KO mice, compared with air-exposed littermates (Fig. 4). In the lung compartment, there were no significant differences between wild-type and CCR6 KO animals, except for the significantly lower numbers of DCs (upon subacute CS exposure) and activated $CD8^+$ T lymphocytes and granulocytes (upon chronic CS exposure) in the CCR6 KO mice (Fig. 4, *B* and *E*). The

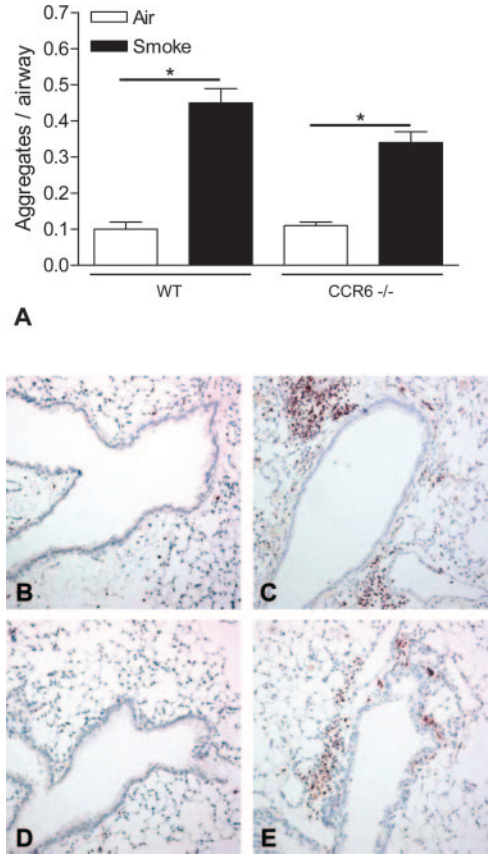

FIGURE 5. Quantification of pulmonary lymphoid aggregates. *A*, Lymphoid aggregates around the airways in lung tissue of wild-type and CCR6 KO mice after chronic (24-wk) exposure to CS, compared with air-exposed mice. Results are expressed as means ± SEM. $n = 8$ animals/group; *, $p < 0.05$. Photomicrographs of lymphoid aggregates in CD3-stained lung tissue of air- and smoke-exposed wild-type and CCR6 KO mice at 24 wk (magnification, ×100). *B*, Air-exposed wild-type mice; *C*, CS-exposed wild-type mice; *D*, air-exposed CCR6 KO mice; and *E*, CS-exposed CCR6 KO mice.

number of B lymphocytes did not change significantly upon smoke exposure (data not shown).

Chronic CS-induced increase in pulmonary lymphoid aggregates

Immunohistochemistry using an anti-CD3 mAb to stain T lymphocytes revealed hardly any lymphoid aggregates in the lung areas surrounding the airways or blood vessels of air-exposed wild-type and CCR6 KO mice. Chronic CS exposure significantly increased the number of peribronchial lymphoid aggregates (which also occur perivascularly) in the lungs of both wild-type and CCR6 KO mice (Fig. 5). However, there was a trend toward less aggregates in the CS-exposed CCR6 KO mice, compared with the wild-type littermates ($p = 0.077$) (Fig. 5*A*). No pulmonary aggregates could be detected in the lungs after subacute CS exposure.

Partial protection against emphysema in CCR6 KO mice upon chronic CS exposure

Pulmonary emphysema is characterized by destruction of alveolar walls due to damage to the lung parenchyma, leading to enlargement of alveolar spaces. Therefore, to quantify emphysematous lesions, it is recommended to evaluate both the airspace enlargement (quantified by the measurement of the L_m) and the destruction of the alveolar walls (quantified by the measurement of the DI).

Chronic CS exposure clearly induced pulmonary emphysema in wild-type mice, evidenced by a significant increase in L_m (air, 41.08 ± 0.33 μm vs smoke, 49.91 ± 0.72 μm; 14.2% increase) and DI (air, 28.12 ± 1.03 vs smoke, 41.92 ± 1.42; 49.1% increase). Also, in CCR6 KO animals, chronic CS exposure led to an induction of emphysema, evidenced by a significant increase in L_m (air, 42.19 ± 0.51 μm vs smoke, 44.19 ± 0.33 μm; 4.7% increase) and DI (air, 27.51 ± 1.44 vs smoke, 33.67 ± 1.64; 22.4% increase). However, the L_m and DI of the smoke-exposed CCR6 KO mice were significantly lower compared with the smoke-exposed wild-type mice (Fig. 6, *A* and *B*), indicating a partial protection against pulmonary emphysema in CCR6 KO mice. The significant airspace enlargement due to chronic CS exposure in wild-type mice and the attenuated emphysema in CCR6 KO mice is illustrated with H&E-stained lung tissue sections (Fig. 6, *C–F*).

Impaired increase in MMP-12 expression in CCR6 KO mice upon CS exposure

MMP-12 is one of the key proteinases implicated in the development of pulmonary emphysema (45). Because CS-induced emphysema is attenuated in CCR6 KO mice, we analyzed the pulmonary expression of MMP-12 by RT-PCR and immunohistochemistry. Subacute CS exposure induced a significant increase in MMP-12 mRNA in both wild-type and CCR6 KO mice, compared with air-exposed littermates. However, the CS-induced increase in MMP-12 mRNA expression was significantly attenuated in the CCR6 KO mice, compared with wild-type animals (Fig. 7*A*). Immunohistochemistry clearly revealed MMP-12 staining in macrophages and DCs of chronic CS-exposed wild-type and CCR6 KO mice, compared with the absence of MMP-12 staining in air-exposed littermates (Fig. 7, *B–E*). Again, the MMP-12 induction seemed attenuated in the CCR6 KO mice, as evidenced by a fainter staining, compared with wild-type mice.

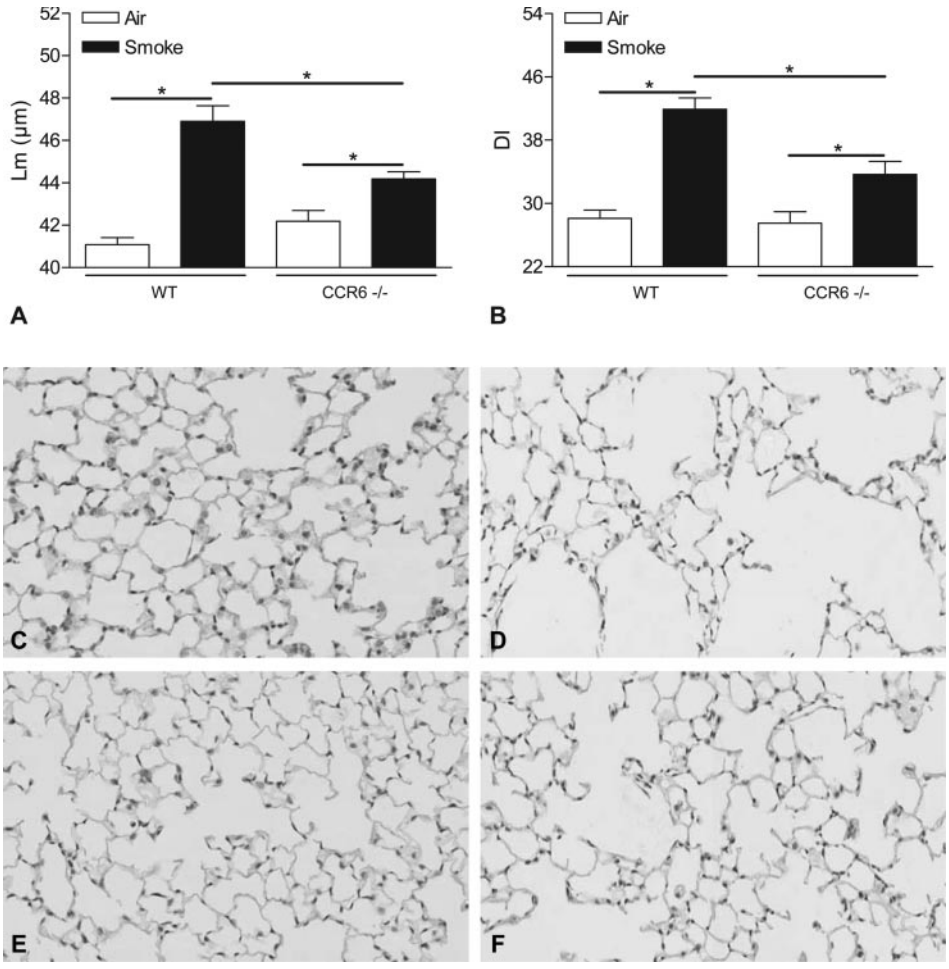

FIGURE 6. Quantification of pulmonary emphysema. Morphometry of the lungs after chronic (24-wk) air or CS exposure: *A*, L_m and *B*, DI values of wild-type and CCR6 KO mice. Results are expressed as means ± SEM. $n = 8$ animals/group; *, $p < 0.05$. Photomicrographs of H&E-stained lung tissue of air- and smoke-exposed wild-type and CCR6 KO mice at 24 wk (magnification, ×200). *C*, Air-exposed wild-type mice; *D*, CS-exposed wild-type mice; *E*, air-exposed CCR6 KO mice; and *F*, CS-exposed CCR6 KO mice.

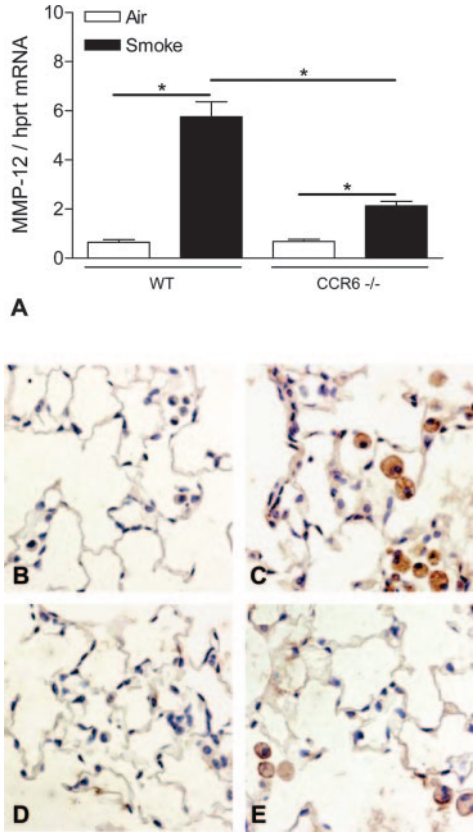

FIGURE 7. Measurement of MMP-12 in lung tissue. *A*, RT-PCR for the expression of MMP-12 mRNA in total lung tissue of wild-type and CCR6 KO mice after subacute (4-wk) exposure to air or CS. Results are expressed as a ratio with hprt mRNA (mean ± SEM). $n = 5$ animals/group; ∗, $p < 0.05$. Immunohistochemistry for MMP-12 protein on lung tissue of wild-type and CCR6 KO mice exposed to air or CS for 24 wk (chronic exposure) (magnification, ×400). MMP-12 is expressed by macrophages and DCs. *B*, Air-exposed wild-type mice; *C*, CS-exposed wild-type mice; *D*, air-exposed CCR6 KO mice; and *E*, CS-exposed CCR6 KO mice. Photomicrographs are representative of eight animals per group.

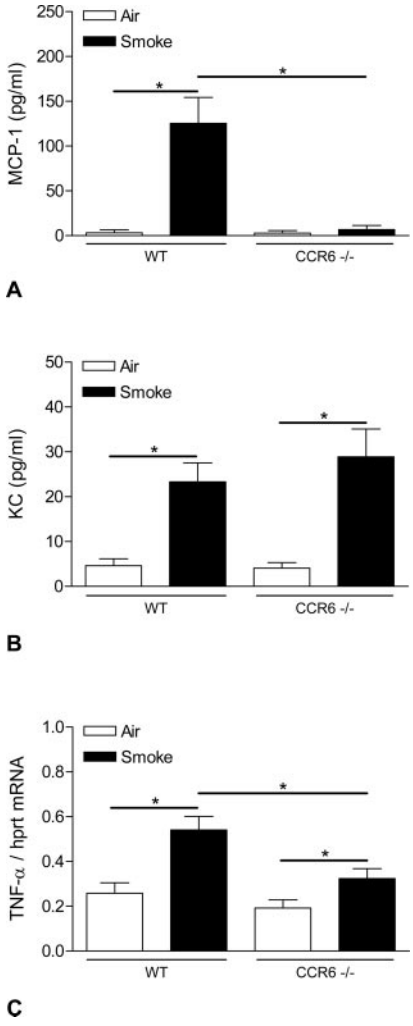

FIGURE 8. Effect of subacute (4-wk) exposure to air or CS on the protein levels of MCP-1 (*A*) and KC (mouse IL-8) (*B*) in BAL fluid of wild-type and CCR6 KO mice, as measured by CBA. Results are expressed as pg/ml (mean ± SEM). $n = 8$ animals/group; ∗, $p < 0.05$. *C*, RT-PCR for the expression of TNF-α mRNA in total lung tissue of wild-type and CCR6 KO mice after subacute (4-wk) exposure to air or CS. Results are expressed as a ratio with hprt mRNA (mean ± SEM). $n = 5$ animals/group; ∗, $p < 0.05$.

Subacute CS-induced increase of inflammatory chemokines and cytokines

To gain further insight in the molecular mechanisms of the attenuated inflammation and emphysema in CCR6 KO mice, we measured protein levels of MCP-1, KC, and TNF-α in the BAL fluid by CBA, as well as the TNF-α mRNA expression in total lung tissue by RT-PCR.

Subacute exposure to CS induced a strong increase in MCP-1 protein in the BAL fluid of wild-type mice, while there was no up-regulation in the CCR6 KO mice (Fig. 8*A*). KC (mouse homolog for IL-8) was increased in BAL fluid of both wild-type and CCR6 KO mice upon subacute CS exposure (Fig. 8*B*).

The levels of TNF-α protein were below detection limit in almost all BAL fluid samples (data not shown), while subacute exposure to CS induced a significant increase in TNF-α mRNA in total lung tissue of wild-type mice, which was significantly attenuated in the CCR6 KO mice (Fig. 8*C*).

Chronic CS-induced airway wall remodeling

To investigate the effects of chronic CS exposure on the deposition of extracellular matrix in the airway wall, lung sections were stained with antifibronectin or Sirius Red to reveal fibronectin and collagen, respectively. In both wild-type and CCR6 KO mice, chronic CS exposure induced a significant increase in peribronchial fibronectin deposition (Fig. 9, *A–E*). Similarly, chronic CS exposure significantly increased the amount of collagen present in the peribronchial area of both wild-type and CCR6 KO mice (Fig. 9, *F–J*). Moreover, this increased deposition of fibronectin and collagen resulted in a significant thickening of the airway wall upon chronic CS exposure in both genotypes (Fig. 9*K*).

Differential cell counts on blood leukocytes upon subacute CS exposure

Because COPD is also characterized by systemic inflammation, we performed differential cell counts on blood leukocytes, distinguishing monocytes, granulocytes, and B and T lymphocytes. Subacute CS exposure significantly increased blood granulocytes (measured as percentage of total blood leukocytes), in both wild-type and CCR6 KO mice (wild type = air, 8.52 ± 1.30% vs CS, 16.16 ± 2.57%, $p < 0.05$; CCR6 KO = air, 8.92% ± 1.91 vs CS, 15.45 ± 1.88%, $p < 0.05$). In contrast, subacute CS exposure did not change the percentage of blood monocytes and B lymphocytes (monocytes: wild type = air, 4.92 ± 0.42% vs CS, 5.33 ± 0.64%,

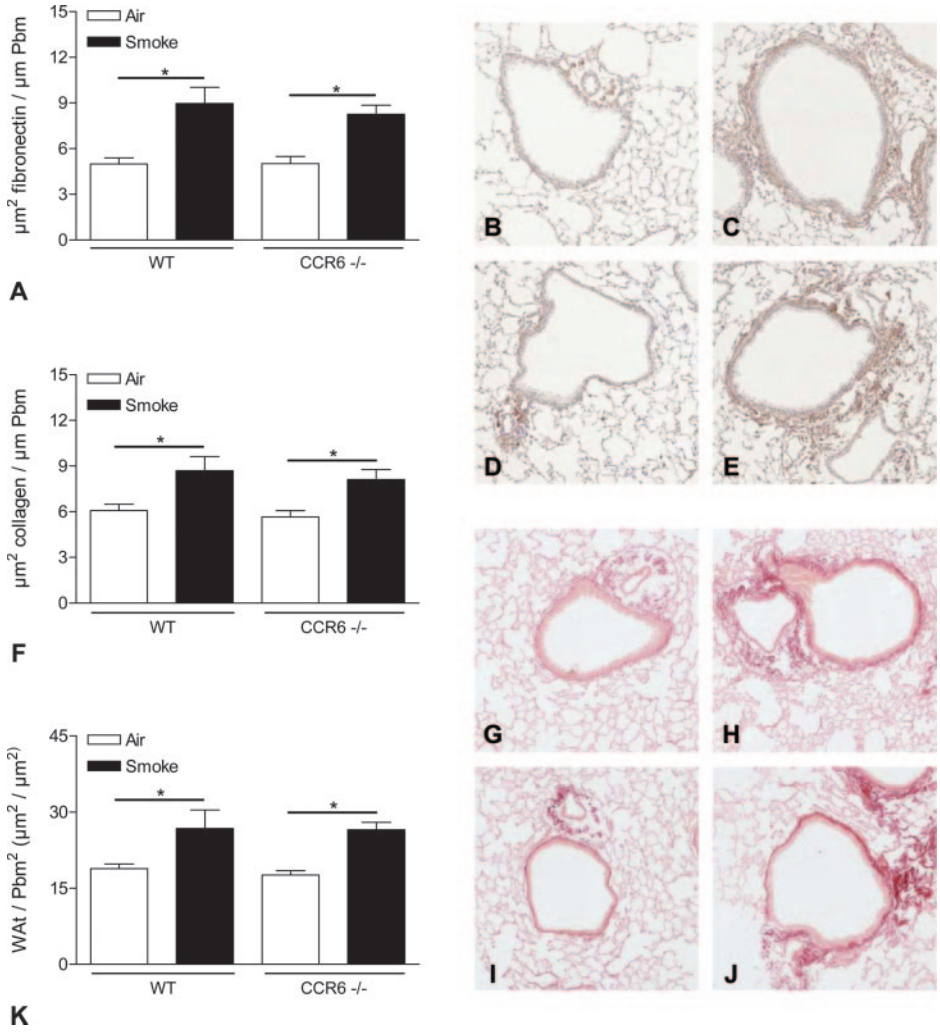

FIGURE 9. Quantification of airway wall remodeling. *A*, Peribronchial fibronectin deposition in lung tissue of wild-type and CCR6 KO mice after chronic (24-wk) exposure to air or CS. Results are expressed as means ± SEM. $n = 8$ animals/group; *, $p < 0.05$. Photomicrographs of peribronchial fibronectin deposition (magnification, ×100): *B*, air-exposed wild-type mice; *C*, CS-exposed wild-type mice; *D*, air-exposed CCR6 KO mice; and *E*, CS-exposed CCR6 KO mice. *F*, Peribronchial collagen deposition in lung tissue of wild-type and CCR6 KO mice after chronic (24-wk) exposure to air or CS. Results are expressed as means ± SEM. $n = 8$ animals/group; *, $p < 0.05$. Photomicrographs of peribronchial collagen deposition (magnification, ×100): *G*, air-exposed wild-type mice; *H*, CS-exposed wild-type mice; *I*, air-exposed CCR6 KO mice; and *J*, CS-exposed CCR6 KO mice. *K*, Airway wall thickness of wild-type and CCR6 KO mice upon chronic (24-wk) exposure to air or CS. Results are expressed as means ± SEM. $n = 8$ animals/group; *, $p < 0.05$.

NS; CCR6 KO = air, 4.62 ± 0.52% vs CS, 4.06 ± 0.58%, NS; B lymphocytes: wild type = air, 49.41 ± 5.83% vs CS, 51.24 ± 1.53%, NS; CCR6 KO = air, 49.58 ± 2.68% vs CS, 44.33 ± 2.85%, NS). Also, on the numbers of T lymphocytes, there was no effect of CS exposure. However, the percentage of T lymphocytes was significantly higher in CCR6 KO mice, compared with wild-type mice (air = wild type, 19.41 ± 1.83% vs CCR6 KO, 29.74 ± 1.51%, $p < 0.01$; smoke = wild type, 19.69 ± 1.19% vs CCR6 KO, 28.97 ± 2.73%, $p < 0.01$).

Discussion

COPD is mainly caused by cigarette smoking, and is characterized by a pulmonary inflammation with an increase in cells of both the innate and the adaptive immune system. In this study, we have demonstrated that the CS-induced pulmonary inflammation is partly impaired in CCR6 KO mice, resulting in an attenuated increase of DCs, T lymphocytes, and neutrophils in the BAL fluid and an impaired increase in DCs, activated $CD8^+$ T lymphocytes, and granulocytes in the lungs of CCR6 KO mice, compared with wild-type littermates. Importantly, upon chronic CS exposure, there was a partial protection against pulmonary emphysema in the CCR6 KO mice. In contrast, CCR6 deficiency had no effect on the development of airway wall remodeling and systemic inflammation.

We have shown that both mRNA and protein levels of MIP-3α/CCL20, the unique chemokine ligand for the CCR6 receptor, are significantly increased upon CS exposure in wild-type mice. This can be due to activation of the lung epithelium, either directly by CS or indirectly via inflammatory mediators such as TNF-α or IFN-γ (34), which are released in the ongoing process of COPD. MIP-3α is known to attract CCR6-expressing cells from the tissue to the site of pathogen invasion (17), and may contribute to the CS-induced pulmonary inflammation. Indeed, in CCR6 KO mice, we observed an attenuated increase in the numbers of DCs and T lymphocytes (cell types that clearly showed CCR6 expression in wild-type mice), whereas the numbers of macrophages (that are not expressing CCR6) were comparable to the wild-type animals. Moreover, in CCR6 KO mice, we observed significantly lower levels of MIP-3α. This can be a downstream effect of the CCR6 deficiency, in which the impaired pulmonary inflammation leads to a reduced release of inflammatory mediators such as TNF-α or IFN-γ, thereby hampering the activation of airway epithelial cells to release MIP-3α.

We also found the chemokine MCP-1 to be strongly induced in CS-exposed wild-type mice. MCP-1 binds to CCR2, a receptor that is highly expressed on circulating blood DCs and monocytes, and thus primarily controls their recruitment from the blood vessels to the tissue (17). In contrast to wild-type mice, there was no increase in MCP-1 levels in CCR6 KO mice upon CS exposure, again probably a downstream effect of the CCR6 deficiency in which the impaired pulmonary inflammation leads to less MCP-1 release.

CS-exposed CCR6 KO mice also showed a significant attenuation in neutrophil influx. This can be due to a direct effect of the

lack of CCR6, which is described to be present on certain cytokine-activated neutrophils (30), or indirectly via the release of other inflammatory mediators. One neutrophil-attracting chemokine that we found to be significantly induced upon CS exposure is KC (the mouse homolog for IL-8), but there were no differences between wild-type and CCR6 KO mice.

The remaining recruitment of DCs, neutrophils, and T lymphocytes to the airways of CCR6 KO mice can be explained by the release of other chemokines, such as MIP-1α/CCL3 or I-TAC/CXCL11, which are also chemotactic for a variety of inflammatory cells by binding to chemokine receptors like CCR5 (46) or CXCR3 (47–49), respectively. Also, elastin fragments, generated as a result of proteolysis of elastin fibers by neutrophil elastase or MMP-12, are chemotactic for monocytes (50). The fact that baseline levels of BAL DCs and lymphocytes were lower in the air-exposed CCR6 KO mice compared with wild-type littermates suggests that the CCR6 pathway is not only important in CS-induced inflammation, but also in the homeostatic recruitment of inflammatory cells to the airways.

The reduced accumulation of DCs in CCR6-deficient mice upon CS exposure supports the findings by Osterholzer et al. (51), who described the contribution of CCR6 to DC migration into alveolar spaces of allergen-challenged mice. In the same respect, Le Borgne et al. (52) showed that recruitment of DCs into epithelial tissues for $CD8^+$ T lymphocyte priming depends on the CCR6/MIP-3α pathway.

The alveolar destruction in pulmonary emphysema is believed to originate mainly from an imbalance between proteinases and their inhibitors. Macrophages are an important source of proteinases, especially MMP-12, which has been implicated in the development of pulmonary emphysema upon long-term CS exposure in mice (45). We have shown recently that not only macrophages, but also DCs are capable of releasing MMP-12 in response to CS (53). The impaired production of MMP-12 that we observed in CS-exposed CCR6 KO mice can be the result of the lower numbers of DCs, or can be due to an attenuated activation of DCs and macrophages in these mice. Either way, these lower levels of MMP-12 can be a possible explanation for the partial protection against alveolar destruction and emphysema in CCR6 KO mice.

Several additional mechanisms might explain why CCR6 KO mice are partially protected against CS-induced pulmonary emphysema. First, neutrophils are another important source of proteinases, releasing serine proteinases such as neutrophil elastase, which is also implicated in the pathogenesis of pulmonary emphysema (15). The lower number of neutrophils in CCR6 KO mice will lead to less neutrophil elastase, further influencing the proteinase/antiproteinase imbalance in CCR6 KO mice. Second, the attenuated smoke-induced increase of T lymphocytes in CCR6 KO mice might also contribute to the partial protection against CS-induced pulmonary emphysema. Indeed, cytotoxic $CD8^+$ T lymphocytes have the capacity to cause cytolysis and apoptosis of alveolar epithelial cells through the release of perforins and granzyme B (19, 54).

Contrary to the clear influence of the CCR6 deficiency on CS-induced pulmonary inflammation and airspace enlargement, it had no effect on airway wall remodeling, another hallmark of COPD. This suggests that the peribronchial deposition of fibronectin and collagen is not a direct downstream effect of the ongoing pulmonary inflammation, but rather occurs through independent processes, a theory that has also been proposed for remodeling in asthma (55, 56). It is not known what exactly drives these processes, but there is evidence for the involvement of TGF-β (57).

COPD is also characterized by systemic inflammation (5, 6). Whether this is the result of spillover from the airway inflammation or not is still controversial. We have shown that the CS-induced increase in blood granulocytes is not influenced by the attenuated pulmonary inflammation in CCR6 KO mice, indicating that CS can directly produce systemic inflammation, as has also been evidenced in human smokers (6).

In conclusion, we have demonstrated that CCR6 deficiency leads to an impaired accumulation of myeloid DCs, neutrophils, and T lymphocytes upon CS exposure, which is reflected in a partial protection against the development of pulmonary emphysema. This indicates that the interaction of CCR6 with its ligand MIP-3α contributes to the pathogenesis of CS-induced pulmonary inflammation and emphysema.

Acknowledgments

We thank Greet Barbier, Eliane Castrique, Indra De Borle, Philippe De Gryze, Katleen De Saedeleer, Marie-Rose Mouton, Ann Neessen, and Christelle Snauwaert for their technical assistance.

Disclosures

The authors have no financial conflict of interest.

References

1. Pauwels, R. A., A. S. Buist, P. M. Calverley, C. R. Jenkins, and S. S. Hurd. 2001. Global strategy for the diagnosis, management, and prevention of chronic obstructive pulmonary disease: NHLBI/WHO Global Initiative for Chronic Obstructive Lung Disease (GOLD) Workshop summary. *Am. J. Respir. Crit. Care Med.* 163: 1256–1276.
2. Murray, C. J., and A. D. Lopez. 1997. Alternative projections of mortality and disability by cause 1990–2020: Global Burden of Disease Study. *Lancet* 349: 1498–1504.
3. Barnes, P. J., S. D. Shapiro, and R. A. Pauwels. 2003. Chronic obstructive pulmonary disease: molecular and cellular mechanisms. *Eur. Respir. J.* 22: 672–688.
4. Jeffery, P. K. 2004. Remodeling and inflammation of bronchi in asthma and chronic obstructive pulmonary disease. *Proc. Am. Thorac. Soc.* 1: 176–183.
5. Vernooy, J. H., M. Kucukaycan, J. A. Jacobs, N. H. Chavannes, W. A. Buurman, M. A. Dentener, and E. F. Wouters. 2002. Local and systemic inflammation in patients with chronic obstructive pulmonary disease: soluble tumor necrosis factor receptors are increased in sputum. *Am. J. Respir. Crit. Care Med.* 166: 1218–1224.
6. Gan, W. Q., S. F. Man, A. Senthilselvan, and D. D. Sin. 2004. Association between chronic obstructive pulmonary disease and systemic inflammation: a systematic review and a meta-analysis. *Thorax* 59: 574–580.
7. Shapiro, S. D. 1999. The macrophage in chronic obstructive pulmonary disease. *Am. J. Respir. Crit. Care Med.* 160: S29–S32.
8. Retamales, I., W. M. Elliott, B. Meshi, H. O. Coxson, P. D. Pare, F. C. Sciurba, R. M. Rogers, S. Hayashi, and J. C. Hogg. 2001. Amplification of inflammation in emphysema and its association with latent adenoviral infection. *Am. J. Respir. Crit. Care Med.* 164: 469–473.
9. Finkelstein, R., R. S. Fraser, H. Ghezzo, and M. G. Cosio. 1995. Alveolar inflammation and its relation to emphysema in smokers. *Am. J. Respir. Crit. Care Med.* 152: 1666–1672.
10. Lacoste, J. Y., J. Bousquet, P. Chanez, T. Van Vyve, J. Simony-Lafontaine, N. Lequeu, P. Vic, I. Enander, P. Godard, and F. B. Michel. 1993. Eosinophilic and neutrophilic inflammation in asthma, chronic bronchitis, and chronic obstructive pulmonary disease. *J. Allergy Clin. Immunol.* 92: 537–548.
11. Casolaro, M. A., J. F. Bernaudin, C. Saltini, V. J. Ferrans, and R. G. Crystal. 1988. Accumulation of Langerhans' cells on the epithelial surface of the lower respiratory tract in normal subjects in association with cigarette smoking. *Am. Rev. Respir. Dis.* 137: 406–411.
12. Soler, P., A. Moreau, F. Basset, and A. J. Hance. 1989. Cigarette smoking-induced changes in the number and differentiated state of pulmonary dendritic cells/Langerhans cells. *Am. Rev. Respir. Dis.* 139: 1112–1117.
13. O'Shaughnessy, T. C., T. W. Ansari, N. C. Barnes, and P. K. Jeffery. 1997. Inflammation in bronchial biopsies of subjects with chronic bronchitis: inverse relationship of $CD8^+$ T lymphocytes with FEV1. *Am. J. Respir. Crit. Care Med.* 155: 852–857.
14. Shapiro, S. D., and R. M. Senior. 1999. Matrix metalloproteinases: matrix degradation and more. *Am. J. Respir. Cell Mol. Biol.* 20: 1100–1102.
15. Shapiro, S. D., N. M. Goldstein, A. M. Houghton, D. K. Kobayashi, D. Kelley, and A. Belaaouaj. 2003. Neutrophil elastase contributes to cigarette smoke-induced emphysema in mice. *Am. J. Pathol.* 163: 2329–2335.
16. Demedts, I. K., G. G. Brusselle, K. R. Bracke, K. Y. Vermaelen, and R. A. Pauwels. 2005. Matrix metalloproteinases in asthma and COPD. *Curr. Opin. Pharmacol.* 5: 257–263.
17. Vanbervliet, B., B. Homey, I. Durand, C. Massacrier, S. Ait-Yahia, O. de Bouteiller, A. Vicari, and C. Caux. 2002. Sequential involvement of CCR2 and CCR6 ligands for immature dendritic cell recruitment: possible role at inflamed epithelial surfaces. *Eur. J. Immunol.* 32: 231–242.

18. Singer, M., and P. J. Sansonetti. 2004. IL-8 is a key chemokine regulating neutrophil recruitment in a new mouse model of *Shigella*-induced colitis. *J. Immunol.* 173: 4197–4206.
19. Cosio, M. G., J. Majo, and M. G. Cosio. 2002. Inflammation of the airways and lung parenchyma in COPD: role of T cells. *Chest* 121: 160S–165S.
20. Taraseviciene-Stewart, L., R. Scerbavicius, K. H. Choe, M. Moore, A. Sullivan, M. R. Nicolls, A. P. Fontenot, R. M. Tuder, and N. F. Voelkel. 2005. An animal model of autoimmune emphysema. *Am. J. Respir. Crit. Care Med.* 171: 734–742.
21. Hogg, J. C., F. Chu, S. Utokaparch, R. Woods, W. M. Elliott, L. Buzatu, R. M. Cherniack, R. M. Rogers, F. C. Sciurba, H. O. Coxson, and P. D. Pare. 2004. The nature of small-airway obstruction in chronic obstructive pulmonary disease. *N. Engl. J. Med.* 350: 2645–2653.
22. D'hulst, A. I., K. Y. Vermaelen, G. G. Brusselle, G. F. Joos, and R. A. Pauwels. 2005. Time course of cigarette smoke-induced pulmonary inflammation in mice. *Eur. Respir. J.* 26: 204–213.
23. D'hulst, A. I., T. Maes, K. R. Bracke, I. K. Demedts, K. G. Tournoy, G. F. Joos, and G. G. Brusselle. 2005. Cigarette smoke-induced pulmonary emphysema in scid-mice: is the acquired immune system required? *Respir. Res.* 6: 147.
24. Van der Strate, B. W., D. S. Postma, C. A. Brandsma, B. N. Melgert, M. A. Luinge, M. Geerlings, M. N. Hylkema, B. A. van den, W. Timens, and H. A. Kerstjens. 2006. Cigarette smoke-induced emphysema: a role for the B cell? *Am. J. Respir. Crit. Care Med.* 173: 751–758.
25. Yoshie, O., T. Imai, and H. Nomiyama. 2001. Chemokines in immunity. *Adv. Immunol.* 78: 57–110.
26. Yang, D., O. Chertov, S. N. Bykovskaia, Q. Chen, M. J. Buffo, J. Shogan, M. Anderson, J. M. Schroder, J. M. Wang, O. M. Howard, and J. J. Oppenheim. 1999. β-Defensins: linking innate and adaptive immunity through dendritic and T cell CCR6. *Science* 286: 525–528.
27. Greaves, D. R., W. Wang, D. J. Dairaghi, M. C. Dieu, B. Saint-Vis, K. Franz-Bacon, D. Rossi, C. Caux, T. McClanahan, S. Gordon, et al. 1997. CCR6, a CC chemokine receptor that interacts with macrophage inflammatory protein 3α and is highly expressed in human dendritic cells. *J. Exp. Med.* 186: 837–844.
28. Krzysiek, R., E. A. Lefevre, J. Bernard, A. Foussat, P. Galanaud, F. Louache, and Y. Richard. 2000. Regulation of CCR6 chemokine receptor expression and responsiveness to macrophage inflammatory protein-3α/CCL20 in human B cells. *Blood* 96: 2338–2345.
29. Liao, F., R. L. Rabin, C. S. Smith, G. Sharma, T. B. Nutman, and J. M. Farber. 1999. CC-chemokine receptor 6 is expressed on diverse memory subsets of T cells and determines responsiveness to macrophage inflammatory protein 3α. *J. Immunol.* 162: 186–194.
30. Yamashiro, S., J. M. Wang, D. Yang, W. H. Gong, H. Kamohara, and T. Yoshimura. 2000. Expression of CCR6 and CD83 by cytokine-activated human neutrophils. *Blood* 96: 3958–3963.
31. Hillyer, P., E. Mordelet, G. Flynn, and D. Male. 2003. Chemokines, chemokine receptors and adhesion molecules on different human endothelia: discriminating the tissue-specific functions that affect leukocyte migration. *Clin. Exp. Immunol.* 134: 431–441.
32. Caux, C., B. Vanbervliet, C. Massacrier, S. Ait-Yahia, C. Vaure, K. Chemin, M. C. Dieu-Nosjean, and A. Vicari. 2002. Regulation of dendritic cell recruitment by chemokines. *Transplantation* 73: S7–S11.
33. Dieu-Nosjean, M. C., C. Massacrier, B. Homey, B. Vanbervliet, J. J. Pin, A. Vicari, S. Lebecque, C. Dezutter-Dambuyant, D. Schmitt, A. Zlotnik, and C. Caux. 2000. Macrophage inflammatory protein 3α is expressed at inflamed epithelial surfaces and is the most potent chemokine known in attracting Langerhans cell precursors. *J. Exp. Med.* 192: 705–718.
34. Reibman, J., Y. Hsu, L. C. Chen, B. Bleck, and T. Gordon. 2003. Airway epithelial cells release MIP-3α/CCL20 in response to cytokines and ambient particulate matter. *Am. J. Respir. Cell Mol. Biol.* 28: 648–654.
35. Hieshima, K., T. Imai, G. Opdenakker, J. Van Damme, J. Kusuda, H. Tei, Y. Sakaki, K. Takatsuki, R. Miura, O. Yoshie, and H. Nomiyama. 1997. Molecular cloning of a novel human CC chemokine liver and activation-regulated chemokine (LARC) expressed in liver: chemotactic activity for lymphocytes and gene localization on chromosome 2. *J. Biol. Chem.* 272: 5846–5853.
36. Lukacs, N. W., D. M. Prosser, M. Wiekowski, S. A. Lira, and D. N. Cook. 2001. Requirement for the chemokine receptor CCR6 in allergic pulmonary inflammation. *J. Exp. Med.* 194: 551–555.
37. Cook, D. N., D. M. Prosser, R. Forster, J. Zhang, N. A. Kuklin, S. J. Abbondanzo, X. D. Niu, S. C. Chen, D. J. Manfra, M. T. Wiekowski, et al. 2000. CCR6 mediates dendritic cell localization, lymphocyte homeostasis, and immune responses in mucosal tissue. *Immunity* 12: 495–503.
38. Macdonald, G., N. Kondor, V. Yousefi, A. Green, F. Wong, and C. Aquino-Parsons. 2004. Reduction of carboxyhaemoglobin levels in the venous blood of cigarette smokers following the administration of carbogen. *Radiother. Oncol.* 73: 367–371.
39. Vermaelen, K. Y., I. Carro-Muino, B. N. Lambrecht, and R. A. Pauwels. 2001. Specific migratory dendritic cells rapidly transport antigen from the airways to the thoracic lymph nodes. *J. Exp. Med.* 193: 51–60.
40. Vermaelen, K., and R. Pauwels. 2004. Accurate and simple discrimination of mouse pulmonary dendritic cell and macrophage populations by flow cytometry: methodology and new insights. *Cytometry* 61A: 170–177.
41. Saetta, M., R. J. Shiner, G. E. Angus, W. D. Kim, N. S. Wang, M. King, H. Ghezzo, and M. G. Cosio. 1985. Destructive index: a measurement of lung parenchymal destruction in smokers. *Am. Rev. Respir. Dis.* 131: 764–769.
42. Thurlbeck, W. M. 1967. Measurement of pulmonary emphysema. *Am. Rev. Respir. Dis.* 95: 752–764.
43. Palmans, E., J. C. Kips, and R. A. Pauwels. 2000. Prolonged allergen exposure induces structural airway changes in sensitized rats. *Am. J. Respir. Crit. Care Med.* 161: 627–635.
44. Bai, A., D. H. Eidelman, J. C. Hogg, A. L. James, R. K. Lambert, M. S. Ludwig, J. Martin, D. M. McDonald, W. A. Mitzner, and M. Okazawa. 1994. Proposed nomenclature for quantifying subdivisions of the bronchial wall. *J. Appl. Physiol.* 77: 1011–1014.
45. Hautamaki, R. D., D. K. Kobayashi, R. M. Senior, and S. D. Shapiro. 1997. Requirement for macrophage elastase for cigarette smoke-induced emphysema in mice. *Science* 277: 2002–2004.
46. Ma, B., M. J. Kang, C. G. Lee, S. Chapoval, W. Liu, Q. Chen, A. J. Coyle, J. M. Lora, D. Picarella, R. J. Homer, and J. A. Elias. 2005. Role of CCR5 in IFN-γ-induced and cigarette smoke-induced emphysema. *J. Clin. Invest.* 115: 3460–3472.
47. Witherden, I. R., E. J. Vanden Bon, P. Goldstraw, C. Ratcliffe, U. Pastorino, and T. D. Tetley. 2004. Primary human alveolar type II epithelial cell chemokine release: effects of cigarette smoke and neutrophil elastase. *Am. J. Respir. Cell Mol. Biol.* 30: 500–509.
48. Panina-Bordignon, P., and D. D'Ambrosio. 2003. Chemokines and their receptors in asthma and chronic obstructive pulmonary disease. *Curr. Opin. Pulm. Med.* 9: 104–110.
49. D'Ambrosio, D., M. Mariani, P. Panina-Bordignon, and F. Sinigaglia. 2001. Chemokines and their receptors guiding T lymphocyte recruitment in lung inflammation. *Am. J. Respir. Crit. Care Med.* 164: 1266–1275.
50. Houghton, A. M., P. A. Quintero, D. L. Perkins, D. K. Kobayashi, D. G. Kelley, L. A. Marconcini, R. P. Mecham, R. M. Senior, and S. D. Shapiro. 2006. Elastin fragments drive disease progression in a murine model of emphysema. *J. Clin. Invest.* 116: 753–759.
51. Osterholzer, J. J., T. Ames, T. Polak, J. Sonstein, B. B. Moore, S. W. Chensue, G. B. Toews, and J. L. Curtis. 2005. CCR2 and CCR6, but not endothelial selectins, mediate the accumulation of immature dendritic cells within the lungs of mice in response to particulate antigen. *J. Immunol.* 175: 874–883.
52. Le Borgne, M., N. Etchart, A. Goubier, S. A. Lira, J. C. Sirard, N. van Rooijen, C. Caux, S. Ait-Yahia, A. Vicari, D. Kaiserlian, and B. Dubois. 2006. Dendritic cells rapidly recruited into epithelial tissues via CCR6/CCL20 are responsible for $CD8^+$ T cell crosspriming in vivo. *Immunity* 24: 191–201.
53. Bracke, K., D. Cataldo, T. Maes, M. Gueders, A. Noel, G. Brusselle, and R. A. Pauwels. 2005. Matrix metalloproteinase-12 and cathepsin D expression in pulmonary macrophages and dendritic cells of cigarette smoking mice. *Int. Arch. Allergy Immunol.* 138: 169–179.
54. Majo, J., H. Ghezzo, and M. G. Cosio. 2001. Lymphocyte population and apoptosis in the lungs of smokers and their relation to emphysema. *Eur. Respir. J.* 17: 946–953.
55. Davies, D. E., J. Wicks, R. M. Powell, S. M. Puddicombe, and S. T. Holgate. 2003. Airway remodeling in asthma: new insights. *J. Allergy Clin. Immunol.* 111: 215–225.
56. Holgate, S. T., J. Holloway, S. Wilson, F. Bucchieri, S. Puddicombe, and D. E. Davies. 2004. Epithelial-mesenchymal communication in the pathogenesis of chronic asthma. *Proc. Am. Thorac. Soc.* 1: 93–98.
57. Wang, R. D., J. L. Wright, and A. Churg. 2005. Transforming growth factor-β1 drives airway remodeling in cigarette smoke-exposed tracheal explants. *Am. J. Respir. Cell Mol. Biol.* 33: 387–393.